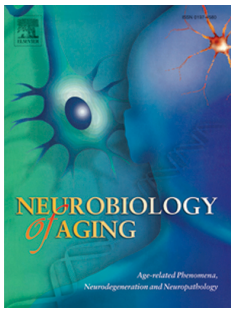

Reduced firing rates of pyramidal cells in the frontal cortex of APP/PS1 can be restored by acute treatment with levetiracetam

Jan L. Klee, Amanda J. Kiliaan, Arto Lipponen, Francesco P. Battaglia

PII: S0197-4580(20)30269-4

DOI: https://doi.org/10.1016/j.neurobiolaging.2020.08.013

Reference: NBA 10929

To appear in: *Neurobiology of Aging*

Received Date: 18 August 2019

Revised Date: 3 August 2020

Accepted Date: 19 August 2020

Please cite this article as: Klee, J.L., Kiliaan, A.J., Lipponen, A., Battaglia, F.P., Reduced firing rates of pyramidal cells in the frontal cortex of APP/PS1 can be restored by acute treatment with levetiracetam, *Neurobiology of Aging* (2020), doi: https://doi.org/10.1016/j.neurobiolaging.2020.08.013.

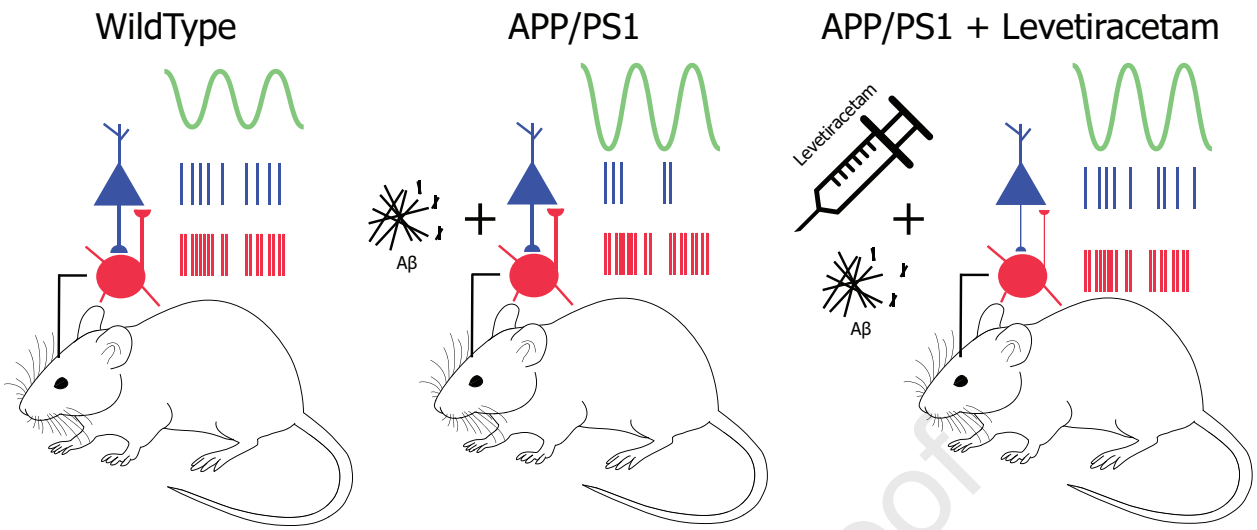

Primary research article

Reduced firing rates of pyramidal cells in the frontal cortex of APP/PS1 can be restored by acute treatment with levetiracetam

Jan L. Klee[1], Amanda J. Kiliaan[2], Arto Lipponen[3]*, Francesco P. Battaglia[1]*

1) Department of Neuroinformatics, Radboud University, Nijmegen, the Netherlands
2) Department of Anatomy, Donders Institute for Brain, Cognition, and Behaviour, Radboud university medical center, Nijmegen, the Netherlands
3) Department of Psychology, University of Jyväskylä, Finland

* equal contribution

Corresponding author

Email Arto.Lipponen@jyu.fi

Tel +358407169558

P.O. Box 35

FIN-40014 University of Jyväskylä

Jyväskylä, Finland

The authors report no conflicts of interest.

Keywords: amyloid, local field potential (LFP), single cell, firing rate, mouse model, Alzheimer's disease

Highlights

- *9 months old APP/PS1 mice exhibit increased theta and beta oscillations in the frontal cortex*

- *Pyramidal cell firing rates are significantly decreased but more phase-locked to ongoing LFP oscillations*

- *Levetiracetam treatment uncouples pyramidal cells and interneurons and elevates pyramidal cell firing rates*

Abstract

In recent years aberrant neural oscillations in various cortical areas have emerged as a common physiological hallmark across mouse models of amyloid pathology and patients with Alzheimer's disease. However, much less is known about the underlying effect of amyloid pathology on single cell activity. Here, we used high density silicon probe recordings from frontal cortex area of 9 months old APP/PS1 mice to show that Local Field Potential (LFP) power in the theta and beta band is increased in transgenic animals, while single cell firing rates, specifically of putative pyramidal cells, are significantly reduced. At the same time, these sparsely firing pyramidal cells phase-lock their spiking activity more strongly to the ongoing theta and beta rhythms. Furthermore, we demonstrated that the anti-epileptic drug, levetiracetam, counteracts these effects by increasing pyramidal cell firing rates in APP/PS1 mice and uncoupling pyramidal cells and interneurons. Overall, our results highlight reduced firing rates of cortical pyramidal cells as a pathophysiological phenotype in APP/PS1 mice and indicate a potentially beneficial effect of acute levetiracetam treatment.

1. Introduction

Network hyper-synchrony and altered neural oscillation have been suggested to contribute to the pathophysiology of Alzheimer's disease (AD) and to the accumulation of AD related amyloid protein (Busche and Konnerth, 2015; Hardy and Selkoe, 2002; Joutsa et al., 2017; Palop and Mucke, 2016). A better understanding of altered neural oscillations in AD could, therefore, provide a target for pharmacological interventions. Even though amyloid plaques and related neuronal loss are among the most significant findings in the post mortem brain of AD patients, the amount of plaques does not correlate with the severity of dementia (Nagy et al., 1995), and the removal of plaques does not lead to an improvement of memory (Holmes et al., 2008). Intriguingly, amyloid accumulation seems to cause excitatory-inhibitory imbalance at the synaptic level, triggering abnormal patterns at both the single cell and network levels which manifest as epileptiform discharges (Minkeviciene et al., 2009). Simultaneously with amyloid plaque formation, both hyper- and hypoactive neurons emerge in the hippocampus and cortical areas (Busche et al., 2012, 2008). Less is known about which subpopulations of cells are affected by amyloid accumulation but it has been proposed that this pathological process is related to persistently decreased resting membrane potential in neocortical pyramidal neurons (Minkeviciene et al., 2009). Similarly, it has been reported that basic biophysical properties of pyramidal neurons in the frontal cortex are intact but external stimulation of these neurons revealed hyper-excitability, indicating a combination of both intrinsic electrical and extrinsic synaptic dysfunctions as mechanisms for activity changes (Kellner et al., 2014). Importantly, aberrant excitatory activity in AD mouse models has also been found to result in a compensatory strengthening of inhibitory circuits which could lead to an overall suppression of neural activity (Palop et al., 2007). Whether these findings apply to in vivo unanesthetized mice, needs to be verified.

On the level of neuronal assemblies, the most prominent finding related to amyloid pathology is abnormally high Local Field Potential (LFP) power over a broad frequency range and during a wide variety of behavioral states (Goutagny et al., 2013; Gurevicius et al., 2013; Jin et al., 2018; Pena-Ortega et al., 2012; Verret et al., 2012), which can lead to epileptiform

synchronous discharges and generalized seizure activity (Gurevicius et al., 2013; Jin et al., 2018; Lam et al., 2017; Minkeviciene et al., 2009; Palop and Mucke, 2016; Vossel et al., 2013). The mechanism by which aberrant single cell activity changes into the generalized epileptiform activity of neuronal ensembles is not clear. Traditionally, epileptic seizures have been characterized as hypersynchrony of large neuronal populations leading to the epileptiform state (Jiruska et al., 2013). However, this view has been challenged by the finding that, during epileptic seizures, there are both increases and decreases in firing rates of neurons, many neurons are unchanged and increased tonic GABAergic inhibition is commonly found in absence epilepsy (Cope et al., 2009; Schevon et al., 2012; Truccolo et al., 2011; Wyler et al., 1982). Furthermore, single cell activity outside the periods of seizures and areas of epileptic foci is more heterogeneous and unsynchronized, and not well characterized (Keller et al., 2010; Truccolo et al., 2011). Also, to our knowledge, it is not known if amyloid accumulation affecting EEG power in a broad frequency band is also entraining single cell activity.

In recent years, antiepileptic pharmacological treatments to balance altered neuronal activity as a consequence of amyloid accumulation have become of interest (Cumbo and Ligori, 2010; Ziyatdinova et al., 2015, 2011). An acute dose of levetiracetam reduces abnormal EEG spiking activity in the cortex and the hippocampus of an AD mouse model for 18 hours after administration (Sanchez et al., 2012). Notably, sub-chronic treatment with levetiracetam has been shown to compensate abnormal hypoactivation in the entorhinal cortex in people with amnestic mild cognitive impairment (aMCI) while simultaneously improving working memory performance (Bakker et al., 2012). Currently, this treatment is under clinical testing although the basic mechanisms of action of levetiracetam in AD patients are not well understood (Bakker et al., 2015). In animal models overexpressing amyloid protein, acute levetiracetam treatment reduces abnormal spike activity, and chronic levetiracetam treatment suppresses hippocampal remodeling, behavioral abnormalities, synaptic dysfunction, and deficits in hippocampal dependent learning and memory (Sanchez et al., 2012). However, levetiracetam has multiple plausible molecular targets including voltage-gated ion currents, synaptic vesicle proteins and the glutaminergic system (Surges et al., 2008), and it is not known which ones are relevant for alleviating AD symptoms.

Current data, however, provide little information about the dynamics of neuronal ensembles that give rise to LFP phenomena, excitatory/inhibitory imbalances as a consequence of amyloid pathology, or on compensatory effects of drugs such as levetiracetam. To investigate these questions, we recorded both LFP and single cell activity in 4 head-fixed APP/PS1 mice and 3 wildtype controls and analyzed the effect of acute levetiracetam treatment. We found that while LFP oscillations showed a power increase in the theta and beta frequency range as previously reported, frontal cortex pyramidal cell firing rates were significantly reduced in APP/PS1 mice. At the same time, the sparsely firing pyramidal cells phase-locked more strongly to the ongoing theta rhythm, Treatment of APP/PS1 mice with levetiracetam specifically elevated pyramidal cell firing rates and uncoupled pyramidal cells and interneurons as shown by decreased pair-wise correlations.

In summary, our results indicate that reduced firing rates of cortical pyramidal cells emerge as a symptom of amyloid pathology and that treatment with levetiracetam might be a viable approach to reverse this abnormal activity.

2. Material and Methods

2.1 Animals

For the present study, we used 4 male $APP_{swe}/PS1_{dE9}$ (APP/PS1) transgenic mice (tg) and 3 age-matched wild type (wt) littermates (all animals underwent the full experiment). The APP/PS1 founder mice were originally obtained from John Hopkins University, Baltimore, MD, USA (D. Borchelt and J. Jankowsky, Department of Pathology) and a colony was first established at the University of Kuopio, Finland. Thereafter a colony was bred at the Central Animal Facility at Radboud University Medical Center, The Netherlands. The mice were created by co-injection of chimeric mouse/human AβPPswe (mouse AβPP695 harbouring a human Aβ domain and mutations K595N and M596L linked to Swedish familial AD pedigrees) and human PS1-dE9 (deletion of exon 9) vectors controlled by independent mouse prion protein promoter elements. The two transfected genes co-integrate and co-segregate as a single locus (Jankowsky et al., 2001). This line was originally maintained on a hybrid background by backcrossing to C3HeJ×C57BL/6J F1 mice (so-called pseudo F2 stage). For the present work, the breeder mice were backcrossed to C57BL/6J for 15 generations to

obtain mice for the current study. The animals were 9 months old at the start of the experiment when animals still do not express memory decline. Interestingly, these mice also display frequent epileptic spiking in the cortex but also the hippocampus, similar to the previous report by Sanchez et al. 2012 but have characteristic abnormal electrophysiological phenotype (Gureviciene et al., 2019). All animals were group housed until the first surgery after which they were individually housed to prevent damage to the implants. Throughout the experiment, the animals received food and water ad libitum and were maintained on a 12-hour light/dark cycle. Recordings were performed during the light period. All experiments were approved by the Dutch governmental Central Commissie Dierproeven (CCD) (10300) and conducted in accordance with the ARRIVE guidelines (Kilkenny et al., 2012).

2.2 Surgical preparation for head-fixed electrophysiological recordings

Animals were anesthetized using isoflurane (0.8 – 1 l/min, 1.5-2 %) and placed in a stereotaxic frame. At the onset of anesthesia, all mice received subcutaneous injections of carprofen (5 mg/kg) as well as a subcutaneous lidocaine injection through the scalp. The animals' temperature was maintained stable for the duration of the surgical procedure using a heating blanket. The level of anesthesia was checked during operation by pedal reflex. We exposed the skull and inserted a skull screw over the cerebellum to serve as combined reference and ground. We then placed a custom made, circular head-plate for head-fixation evenly on the skull and fixated it with dental cement (Super-Bond C&B, Sun Medical, Shiga, Japan). A small craniotomy of about 500µm in diameter was drilled over left frontal cortex at +1.78mm anterior and 0.4 mm lateral to Bregma. The dura mater was left intact and the craniotomy, as well as the rest of the exposed skull, were directly covered with a silicone elastomer (Body Double Fast Set – Trial Size, Reynolds Advanced Materials) until the first recording. All mice were given at least 2 days to recover from the surgery.

2.3 Electrophysiological recordings in the frontal cortex of head-fixed mice

The head-fixation setup consisted of two rods that were screwed onto either side of the implanted head-plate and fixated the mice in place on top of a styrofoam ball that functioned as an air-supported spherical treadmill and allowed us to read out the movement

of the animals in a subset of recording sessions. All animals were slowly habituated to head-fixation by placing them in the setup for 3 sessions of 10 minutes for two days before the first recording day.

Two hours before each recording session, we injected the animals with either 200 mg/kg i.p. levetiracetam, (Sigma-Aldrich, Taufkirchen, Germany), a dose shown to reduce abnormal hyperactivity EEG effectively, or saline (control) (Sanchez et al., 2012). We alternated these injections for 4 consecutive days to be able to record two sessions per animal and condition. However, during 6 of the later sessions, we weren't able to obtain high quality single cell recordings either due to a systems malfunction or a gradual development of scar tissue around the recording sites. We excluded these sessions from the analysis. The experimenter was blind to both the genotype as well as to the type of treatment (levetiracetam or saline)."

At the start of each recording session, we placed the mice in head-fixation and removed the silicone elastomer cover to expose the craniotomy over the frontal cortex. We then used a micromanipulator (Thorlabs, Newton, New Jersey, USA) to acutely insert a 128 channel silicon probe (IMEC, Leuven, Belgium) first -1.5mm and then -2.5mm into the frontal cortex. At each depth, we waited about 15 minutes for the tissue to settle. We then performed 10 minutes of broadband recordings.

Electrophysiological signals were, digitized at 30 kHz using two digitizing headstages (RHD2164 Amplifier Board, Intan Technologies, Los Angeles, California, USA), filtered between 1 and 6000 Hz, and acquired with an open-ephys recording system (Siegle et al., 2017). After each recording session, we retracted the silicon probe and placed a new silicone cover on the skull before releasing the animals back to their respective home cages.

2.4 Histology

At the end of the experiment, the animals were deeply anesthetized with pentobarbital (Nembutal, pentobarbital sodium 60 mg/ml, 65 mg/kg, i.p.) and perfused with 0.1 M phosphate buffer (pH = 7.4.) followed by 4% paraformaldehyde solution for 9 min at 10 mL/min. The brain was removed and immersion postfixated for 4 h in 4% paraformaldehyde

(pH = 7.4) at 4˚C. The brains were thereafter stored at 0.1. phosphate buffer (pH = 7.4) at 4˚C until slicing. Coronal sections (thickness 30 µm) were cut with a freezing slide microtome. Every second section containing a track from the recording electrode were stained for the N-terminal human Aβ-specific antibody W02 (Genetics, Switzerland) to visualize diffuse amyloid deposits as described previously (Hooijmans et al., 2007) to verify the amyloid pathology in the transgenic animals (Fig. 1.). Additionally, we performed a cresyl-violet staining to verify the anterior-posterior coordinates of the recording sites.

2.5 Data analysis

For LFP analysis, we only used the central channel of our recording electrode. We down-sampled the broadband signal to 2000 Hz and then low-pass filtered below 500 Hz. Time-frequency analysis was performed via Morlet wavelet convolution based on the fast Fourier transform (Cohen, 2014). To minimize the effect of movement on our results, we split each recording session into 4-s bins and focused our subsequent analysis on the 20 bins with the highest theta power. Significant differences in the power spectra were calculated using a permutation test at each frequency.

To identify single units, data were automatically spike sorted with Kilosort (Pachitariu et al., 2016) (https://github.com/cortex-lab/Kilosort) and then manually inspected with the phy software (https://github.com/kwikteam/phy). All following analyses were performed using custom written MATLAB scripts. As a post-hoc criterion for the quality of our spike sorting, we computed the auto-correlograms of each putative single unit and only further analyzed cells with less than 2% of spikes within the physiological refractory period of 2ms.

For each unit, we then computed the peak-to-peak amplitude of the action potential waveforms as well as the width at 30% of the negative peak. We fed these values into Gaussian-mixture model to classify single units into putative interneurons with narrower spike waveforms and putative pyramidal cells with broader spike waveform (see Fig. 3 for cut off criteria) (Stark et al., 2013). In contrast to Stark et al., we used the width of the spike waveform at 30% (instead of 50%) of the negative peak because visual inspection of all spike waveform indicated a better separation of putative pyramidal and interneuron waveforms

closer to the base of the waveforms than in at 50% (see Fig.3 A). In total, we identified 1394 single neurons for further analysis.

For each unit, we computed the mean firing rate over the 10-min recording sessions and performed a 3-factorial ANOVA with neuron type, genotype and drug condition as independent variables, followed by post-hoc t-tests whenever justified by significant main or interaction effects.

Additionally, we computed the spike-time cross-correlations between all simultaneously recorded neurons using the binned spike trains (5ms bins, corrcoef function, MATLAB). We then performed a 3-factorial ANOVA with neuron type (in this case pyramidal-pyramidal, interneuron-interneuron and pyramidal-interneuron), genotype and drug condition as independent variables, followed by post-hoc t-tests whenever justified by significant main or interaction effects. (Moore et al., 1966; Perkel et al., 1967a, 1967b). For theta and beta phase locking analysis, we first filtered the raw signal between 4-12 Hz and 12-30 Hz respectively using a zero-lag band-pass filter (filtfilt function, MATLAB) and then extracted the phase angles using the Hilbert transform (hilbert function and angle function, MATLAB). For each putative single cell, we extracted the theta and beta phase angles at each spike and computed the mean resultant length (circ_r function, circular statistic toolbox, MATLAB). In order to determine if spikes were non- uniformly distributed across different phases of the ongoing oscillations, we computed the Rayleigh test for circular uniformity of the spike-phase angles for every cell (circ_rtest function, circular statistic toolbox, MATLAB).

3. Results

3.1 Increased LFP power in 6-26 Hz band in APP/PS1 mice

We recorded both local field potential as well as single cell activity with a 128-channel silicon probe in the frontal cortex of 9-month-old awake, head-fixed APP/PS1 mice and wild type littermate controls (Fig. 1). We found increased theta and beta LFP power between 6 and 26 Hz in the frontal cortex neurons of APP/PS1 mice (saline injected APP/PS1 n=4 mice, 6

sessions; saline injected WT n=3 mice, 4 sessions; permutation test at each frequency $p<0.05$) (Fig. 2.).

3.2 Reduced single cell firing rates in the frontal cortex of APP/PS1 mice

To test how increased LFP power in the theta and beta frequencies relate to the firing rates of individual neurons, we performed single cell recordings from the frontal cortex of APP/PS1 mice. Surprisingly, we found that APP/PS1 mice showed overall reduced firing rates compared to wildtype controls (n= 422 APP/PS1, n= 255 wt; *t*-test, p = 0.01).

To further investigate whether this effect was specific to a certain neuron type, we classified the recorded single cells as either putative pyramidal cells or interneurons according to their action potential waveform (Fig. 3 A & B) (Stark et al., 2013). This analysis revealed that the reduction of firing rates in APP/PS1 mice was statistically significant only for putative pyramidal cells (ANOVA genotype-neurontype interaction $F(1,1427)=5.99$, $p=0.01$; post hoc *t*-test for APP/PS1 (n=372) vs WT pyramidal cells (n=219), p=0.006, ~21% reduction in mean firing rates) while interneurons were not significantly affected (post hoc *t*-test for APP/PS1 (n=50) vs WT (n=36) interneurons, p=.7, ~7% decrease in mean firing rates (Fig. 3 C & D).

3.3 Increased theta and beta phase locking of pyramidal cells in APP/PS1 mice

Our analysis of LFP and single cell activity in APP/PS1 mice points towards the non-trivial relationship between increased local field potential oscillations in the theta and beta range and the underlying single cell firing rates. To shed light on this issue, we made use of our simultaneous LFP and unit recordings and analyzed the entrainment of putative pyramidal cells to the predominant ongoing LFP oscillation in the 4-12 Hz theta and 12-30 Hz beta range. To this end, we filtered the raw LFP signal between 4-12 Hz and 12-30 Hz, respectively, and then computed the phase angles using the Hilbert transform. For each putative single cell, we extracted the theta and beta phase angles for each spike and computed the mean resultant length. We found that the overall more sparsely firing pyramidal cells in APP/PS1 mice were significantly more phase-locked to the ongoing theta and beta oscillation than in wild type controls and clustered around the rising phase of the

theta oscillation (theta: Wilcoxon Rank sum test, $p<0.001$ (Fig. 4A and 4B.); beta: Wilcoxon Rank sum test, $p<0.001$ (Fig. 4C.); n=227 (WT/Pyr); n=386 (APP/PS1/Pyr)). Phase locking in the gamma range between 30-100 Hz was not significantly affected (gamma: Wilcoxon Rank sum test, $p=0.75$, Fig. 4D.).

3.4 Levetiracetam restores reduced firing rates of single neurons in the frontal cortex of APP/PS1 mice

Interestingly, we found that levetiracetam specifically elevated firing rates in frontal cortex neurons in APP/PS1 mice while firing rates in wildtype animals were not significantly affected (genotype by drug interaction $F(1,1427)=7.79$, $p=0.005$; post hoc *t*-test for APP/PS1 cells + lev (n=365) vs APP/PS1 cells + sal (n=431), $p<0.001$) Importantly, classifying cells into putative pyramidal cells and interneurons according to their action potential waveforms revealed that this effect was specific for pyramidal cells (neuron type by drug interaction $F(1,1427)=3.91$, $p=0.048$; post hoc *t*-test for APP/PS1 pyramidal cells + lev (n=326) vs APP/PS1 pyramidal cells + sal (386), $p=0.001$ (Fig. 5 A & B)). We did not find any effect of levetiracetam on average firing rates on either pyramidal cells or interneurons in wildtype animals (*t*-test for WT + lev (n=370) vs WT + sal (262), $p=0.85$) (Fig. 5 A).

3.5 Levetiracetam uncouples pyramidal cells and interneurons in APP/PS1 mice

Levetiracetam has been shown to suppress vesicle release (De Smedt et al., 2007; Surges et al., 2008; Vogl et al., 2012). Therefore, increased firing rates of pyramidal cells in APP/PS1 after treatment with levetiracetam seems more likely to be the result of reduced inhibition rather than a direct stimulating effect on pyramidal cells. To test this hypothesis, we analyzed the pair-wise correlations of all simultaneously recorded single cells in APP/PS1 mice (Fig. 5 C & D). In line with its overall positive effect on single cell firing rates, levetiracetam significantly increased pair-wise pyramidal cell correlations in APP/PS1 mice (Fig. 5 D). In addition, we specifically analyzed correlations between cell pairs that consisted of one pyramidal cell and one interneuron in order to clarify the effect on levetiracetam on the interactions between these cell-types. We found that levetiracetam significantly reduces pyramidal-interneuron correlations in APP/PS1 mice (Fig. 5 D) (three-way interaction

between genotype, neuron type and drug F(3,50291)=.643, p=0.002; post hoc *t*-test for APP/PS1 pyramidal cells + lev (n=9751) vs APP/PS1 pyramidal cells + Sal (n=14724), $p<0.001$; APP/PS1 interneurons + lev (n=93) vs APP/PS1 interneurons + sal (n=165), $p< 0.001$; APP/PS1 pyramidal/interneuron + lev (n=1080) vs APP/PS1 pyramidal/interneurons + sal (n=1260), $p< 0.001$).

4. Discussion

Amyloid pathology has been shown to influence the balance between inhibition and excitation at the level of individual cells and synapses in vitro by modulating both glutamatergic as well as GABAergic neurotransmission at different stages during disease progression (Busche et al., 2012; Minkeviciene et al., 2009; Palop et al., 2007; Zott et al., 2019). Similarly, at the network level, the power of cortical LFP oscillations has previously been reported to be increased in mouse models of Alzheimer's disease and this increase in LFP power has been thought to reflect an impairment in the balance of cortical inhibition and excitation in these animals (Gurevicius et al., 2013; Jin et al., 2018). However, only very few studies have reported recordings from single neurons in awake behaving animals with amyloid pathology (Cacucci et al., 2008; Jun et al., 2019). Our understanding of how exactly changes at excitatory and inhibitory synapses translate into pathologically changed network activity that can be detected with intracranial LFP or EEG recordings has therefore been very limited.

In this context, our data obtained from simultaneous single cell and LFP recordings from the frontal cortex of 9-month-old amyloid expressing APP/PS1 mice has revealed some unexpected new insights. In line with previous studies, we found that LFP power was increased in 9-month-old APP/PS1 mice in the theta and beta frequency bands between 6 and 26 Hz (Gurevicius et al., 2013; Jin et al., 2018). However, our simultaneous recordings of single cell activity and LFP allowed us to go one step further and analyze single cell firing rates as well as the precise temporal relationship between action potential firing of individual cortical neurons and the ongoing LFP oscillations.

Our data suggest that increased LFP power is likely linked to more synchronized spiking of cortical neurons instead of increased overall levels of excitability that had previously been postulated (Gurevicius et al., 2013; Palop and Mucke, 2016). In fact, we found that individual pyramidal cells in APP/PS1 mice have significantly reduced firing rates compared to wildtype controls but phase-lock their activity more strongly to the ongoing LFP oscillations in the beta and theta frequency bands. This overall suppressive effect on firing rates was a surprise to us because several well established lines of evidence have previously shown that one of the primary effects of soluble amyloid beta in APP/PS1 mice is an increase in excitation on the level of individual cells (Minkeviciene et al., 2009). On the single cell level, the amyloid beta protein was shown to directly increase the excitability of cortical pyramidal cells, and cortical cells near amyloid plaques were shown to be hyperactive in anaesthetized animals (Busche et al., 2008; Minkeviciene et al., 2009). However, previous evidence also suggests that at the network level, likely as a response to this direct excitation caused by amyloid beta, hippocampal circuits seem to develop a secondary compensatory mechanism which is characterized by chronically elevated inhibition (Palop et al., 2007). We hypothesis that a similar principle could apply to cortical circuits in APP/PS1 mice.

In support of this view, it has been found that many cortical neurons in anaesthetized AD mice that are further away from plaques have reduced firing rates. Blocking GABAergic inhibition with the GABA A receptor antagonist gabazine drastically increases the firing rates of these neurons (Busche et al., 2008). Furthermore, it has been found that immunoreactivity against GABAa receptor subunit a1 is significantly elevated in APP/PS1 mice suggesting an increase in postsynaptic inhibition in these animals (Yoshiike et al., 2008). Finally, the increased likelihood of epileptic seizures in mouse models and patients with AD has previously been interpreted as a sign for increased cortical excitation instead of inhibition, however, there is also evidence suggesting that GABAa mediated tonic inhibition can be increased in typical absence epilepsy (Cope et al., 2009; Palop and Mucke, 2016). Given these multiple factors that influence single cell activity in AD mouse models, a more detailed electrophysiological characterization, ideally across multiple time-points during pathology progression, different brain regions and with a higher subject count to account for inter-animal differences seems ultimately necessary.

This is particularly relevant because our finding that APP/PS1 mice have overall reduced firing rates of individual cortical pyramidal cells could have important consequences for potential therapeutic strategies. To shed light on this issue, we combined single cell recordings in APP/PS1 mice and treatment with the antiepileptic drug levetiracetam which has been shown to have various positive effects on Alzheimer´s disease pathology and which has previously been hypothesized to exert these positive effects by reducing neuronal activity (Bakker et al., 2012; Palop and Mucke, 2016; Sanchez et al., 2012). However, we found that the mechanisms by which levetiracetam exerts its positive effects during the treatment of epilepsy and Alzheimer's disease might be more complicated. This likely includes both reducing pathologically high inhibition during the non-epileptic state in Alzheimer's disease and reducing aberrant excitation only if and when seizures occur. We revealed that contrary to the idea that levetiracetam exerts its positive effect in Alzheimer's disease by reducing excitability, treatment of APP/PS1 mice with levetiracetam in fact leads to increased firing rates of cortical pyramidal cells. Levetiracetam is known to interact with the synaptic vesicle protein SV2a which is found in both excitatory and inhibitory synapses regulating neurotransmitter release (Vogl et al., 2012). Notably, disruption of SV2a function has been shown to reduce GABA release from inhibitory synapses (Crowder et al., 1999). In line with these findings, we show that levetiracetam treatment leads to an uncoupling of inhibitory interneurons and pyramidal cells in APP/PS1 mice as well as to increased firing of pyramidal cells without affecting interneuron firing rates.

An important question that arises from this interpretation is that if levetiracetam increases excitation by lifting inhibition, why does it not result in an increase in seizures but instead acts as an effective antiepileptic agent? One possible explanation for this is the finding that levetiracetam acts on both inhibitory and excitatory synapses and that it has been shown to reduce excitatory transmitter release at glutamatergic synapses in an activity dependent manner (Yang et al., 2007). Specifically, it was found that at excitatory synapses levetiracetam reduces the size of repeated excitatory postsynaptic potentials but only during high frequency stimulation (Meehan et al., 2011; Yang et al., 2007). This frequency dependency is likely to be the key to the positive effects of levetiracetam which seems to have relatively little influence on the excitatory transmission during normal, physiological

levels of brain activity but has the potential to successfully reduces aberrant firing in a frequency dependent manner during developing seizures.

However, future studies, combining simultaneous single cell recordings and levetiracetam treatment during behavioural testing in amyloid protein expressing mice, will be necessary to conclusively clarify if levetiracetam exerts its positive influence on cognitive function in mouse models and patients with Alzheimer's disease primarily through lifting inhibition or though blocking seizure activity.

Acknowledgements

We thank Prof. Heikki Tanila for helpful comments on the manuscript and Jos Dederen and Vivienne Verweij for excellent technical support. The study was supported by the Säätiöiden post doc -pooli (The Finnish Cultural Foundation) to Dr. Arto Lipponen. Silicon probes were manufactured by IMEC (Leuven, Belgium) with funding from the European Union's Seventh Framework Programme (FP7/2007-2013) under grant agreement nr. 600925 (NeuroSeeker).

References

Bakker, A., Albert, M.S., Krauss, G., Speck, C.L., Gallagher, M., 2015. Response of the medial temporal lobe network in amnestic mild cognitive impairment to therapeutic intervention assessed by fMRI and memory task performance. Neuroimage Clin 7, 688–698. https://doi.org/10.1016/j.nicl.2015.02.009

Bakker, A., Krauss, G.L., Albert, M.S., Speck, C.L., Jones, L.R., Stark, C.E., Yassa, M.A., Bassett, S.S., Shelton, A.L., Gallagher, M., 2012. Reduction of hippocampal hyperactivity improves cognition in amnestic mild cognitive impairment. Neuron 74, 467–474. https://doi.org/10.1016/j.neuron.2012.03.023

Busche, M.A., Chen, X., Henning, H.A., Reichwald, J., Staufenbiel, M., Sakmann, B., Konnerth, A., 2012. Critical role of soluble amyloid-β for early hippocampal hyperactivity in a mouse model of Alzheimer's disease. Proc. Natl. Acad. Sci. U.S.A. 109, 8740–8745. https://doi.org/10.1073/pnas.1206171109

Busche, M.A., Eichhoff, G., Adelsberger, H., Abramowski, D., Wiederhold, K.-H., Haass, C., Staufenbiel, M., Konnerth, A., Garaschuk, O., 2008. Clusters of hyperactive neurons near amyloid plaques in a mouse model of Alzheimer's disease. Science 321, 1686–1689. https://doi.org/10.1126/science.1162844

Busche, M.A., Konnerth, A., 2015. Neuronal hyperactivity--A key defect in Alzheimer's disease? Bioessays 37, 624–632. https://doi.org/10.1002/bies.201500004

Cacucci, F., Yi, M., Wills, T.J., Chapman, P., O'Keefe, J., 2008. Place cell firing correlates with memory deficits and amyloid plaque burden in Tg2576 Alzheimer mouse model. Proc. Natl. Acad. Sci. U.S.A. 105, 7863–7868. https://doi.org/10.1073/pnas.0802908105

Cohen, M.X., 2014. Analyzing neural time series data: theory and practice, Issues in clinical and cognitive neuropsychology. The MIT Press, Cambridge, Massachusetts.

Cope, D.W., Di Giovanni, G., Fyson, S.J., Orbán, G., Errington, A.C., Lorincz, M.L., Gould, T.M., Carter, D.A., Crunelli, V., 2009. Enhanced tonic GABAA inhibition in typical absence epilepsy. Nat. Med. 15, 1392–1398. https://doi.org/10.1038/nm.2058

Crowder, K.M., Gunther, J.M., Jones, T.A., Hale, B.D., Zhang, H.Z., Peterson, M.R., Scheller, R.H., Chavkin, C., Bajjalieh, S.M., 1999. Abnormal neurotransmission in mice lacking synaptic vesicle protein 2A (SV2A). Proc. Natl. Acad. Sci. U.S.A. 96, 15268–15273. https://doi.org/10.1073/pnas.96.26.15268

Cumbo, E., Ligori, L.D., 2010. Levetiracetam, lamotrigine, and phenobarbital in patients with epileptic seizures and Alzheimer's disease. Epilepsy Behav 17, 461–466. https://doi.org/10.1016/j.yebeh.2010.01.015

De Smedt, T., Raedt, R., Vonck, K., Boon, P., 2007. Levetiracetam: the profile of a novel anticonvulsant drug-part I: preclinical data. CNS Drug Rev 13, 43–56. https://doi.org/10.1111/j.1527-3458.2007.00004.x

Goutagny, R., Gu, N., Cavanagh, C., Jackson, J., Chabot, J.-G., Quirion, R., Krantic, S., Williams, S., 2013. Alterations in hippocampal network oscillations and theta-gamma coupling arise before Aβ overproduction in a mouse model of Alzheimer's disease. Eur. J. Neurosci. 37, 1896–1902. https://doi.org/10.1111/ejn.12233

Gureviciene, I., Ishchenko, I., Ziyatdinova, S., Jin, N., Lipponen, A., Gurevicius, K., Tanila, H., 2019. Characterization of Epileptic Spiking Associated With Brain Amyloidosis in APP/PS1 Mice. Front Neurol 10, 1151. https://doi.org/10.3389/fneur.2019.01151

Gurevicius, K., Lipponen, A., Tanila, H., 2013. Increased cortical and thalamic excitability in freely moving APPswe/PS1dE9 mice modeling epileptic activity associated with Alzheimer's disease. Cereb. Cortex 23, 1148–1158. https://doi.org/10.1093/cercor/bhs105

Hardy, J., Selkoe, D.J., 2002. The amyloid hypothesis of Alzheimer's disease: progress and problems on the road to therapeutics. Science 297, 353–356. https://doi.org/10.1126/science.1072994

Holmes, C., Boche, D., Wilkinson, D., Yadegarfar, G., Hopkins, V., Bayer, A., Jones, R.W., Bullock, R., Love, S., Neal, J.W., Zotova, E., Nicoll, J.A.R., 2008. Long-term effects of Abeta42 immunisation in Alzheimer's disease: follow-up of a randomised, placebo-controlled phase I trial. Lancet 372, 216–223. https://doi.org/10.1016/S0140-6736(08)61075-2

Hooijmans, C.R., Graven, C., Dederen, P.J., Tanila, H., van Groen, T., Kiliaan, A.J., 2007. Amyloid beta deposition is related to decreased glucose transporter-1 levels and hippocampal atrophy in brains of aged APP/PS1 mice. Brain Res. 1181, 93–103. https://doi.org/10.1016/j.brainres.2007.08.063

Jankowsky, J.L., Slunt, H.H., Ratovitski, T., Jenkins, N.A., Copeland, N.G., Borchelt, D.R., 2001. Co-expression of multiple transgenes in mouse CNS: a comparison of strategies. Biomol. Eng. 17, 157–165.

Jin, N., Lipponen, A., Koivisto, H., Gurevicius, K., Tanila, H., 2018. Increased cortical beta power and spike-wave discharges in middle-aged APP/PS1 mice. Neurobiol. Aging 71, 127–141. https://doi.org/10.1016/j.neurobiolaging.2018.07.009

Jiruska, P., de Curtis, M., Jefferys, J.G.R., Schevon, C.A., Schiff, S.J., Schindler, K., 2013. Synchronization and desynchronization in epilepsy: controversies and hypotheses. J. Physiol. (Lond.) 591, 787–797. https://doi.org/10.1113/jphysiol.2012.239590

Joutsa, J., Rinne, J.O., Hermann, B., Karrasch, M., Anttinen, A., Shinnar, S., Sillanpää, M., 2017. Association Between Childhood-Onset Epilepsy and Amyloid Burden 5 Decades Later. JAMA Neurol 74, 583–590. https://doi.org/10.1001/jamaneurol.2016.6091

Jun, H., Soma, S., Saito, T., Saido, T.C., Igarashi, K.M., 2019. Disrupted remapping of place cells and grid cells in knock-in model of Alzheimer's disease. bioRxiv 815993. https://doi.org/10.1101/815993

Keller, C.J., Truccolo, W., Gale, J.T., Eskandar, E., Thesen, T., Carlson, C., Devinsky, O., Kuzniecky, R., Doyle, W.K., Madsen, J.R., Schomer, D.L., Mehta, A.D., Brown, E.N., Hochberg, L.R., Ulbert, I., Halgren, E., Cash, S.S., 2010. Heterogeneous neuronal firing patterns during interictal epileptiform discharges in the human cortex. Brain 133, 1668–1681. https://doi.org/10.1093/brain/awq112

Kellner, V., Menkes-Caspi, N., Beker, S., Stern, E.A., 2014. Amyloid-β alters ongoing neuronal activity and excitability in the frontal cortex. Neurobiology of Aging 35, 1982–1991. https://doi.org/10.1016/j.neurobiolaging.2014.04.001

Kilkenny, C., Browne, W.J., Cuthill, I.C., Emerson, M., Altman, D.G., 2012. Improving bioscience research reporting: the ARRIVE guidelines for reporting animal research. Osteoarthr. Cartil. 20, 256–260. https://doi.org/10.1016/j.joca.2012.02.010

Lam, A.D., Deck, G., Goldman, A., Eskandar, E.N., Noebels, J., Cole, A.J., 2017. Silent hippocampal seizures and spikes identified by foramen ovale electrodes in Alzheimer's disease. Nat. Med. 23, 678–680. https://doi.org/10.1038/nm.4330

Meehan, A.L., Yang, X., McAdams, B.D., Yuan, L., Rothman, S.M., 2011. A new mechanism for antiepileptic drug action: vesicular entry may mediate the effects of levetiracetam. J. Neurophysiol. 106, 1227–1239. https://doi.org/10.1152/jn.00279.2011

Minkeviciene, R., Rheims, S., Dobszay, M.B., Zilberter, M., Hartikainen, J., Fülöp, L., Penke, B., Zilberter, Y., Harkany, T., Pitkänen, A., Tanila, H., 2009. Amyloid beta-induced neuronal hyperexcitability triggers progressive epilepsy. J. Neurosci. 29, 3453–3462. https://doi.org/10.1523/JNEUROSCI.5215-08.2009

Moore, G.P., Perkel, D.H., Segundo, J.P., 1966. Statistical analysis and functional interpretation of neuronal spike data. Annu. Rev. Physiol. 28, 493–522. https://doi.org/10.1146/annurev.ph.28.030166.002425

Nagy, Z., Esiri, M.M., Jobst, K.A., Morris, J.H., King, E.M.-F., McDonald, B., Litchfield, S., Smith, A., Barnetson, L., Smith, A.D., 1995. Relative Roles of Plaques and Tangles in the Dementia of Alzheimer's Disease: Correlations Using Three Sets of Neuropathological Criteria. Dementia and Geriatric Cognitive Disorders 6, 21–31. https://doi.org/10.1159/000106918

Palop, J.J., Chin, J., Roberson, E.D., Wang, J., Thwin, M.T., Bien-Ly, N., Yoo, J., Ho, K.O., Yu, G.-Q., Kreitzer, A., Finkbeiner, S., Noebels, J.L., Mucke, L., 2007. Aberrant excitatory neuronal activity and compensatory remodeling of inhibitory hippocampal circuits in mouse models of Alzheimer's disease. Neuron 55, 697–711. https://doi.org/10.1016/j.neuron.2007.07.025

Palop, J.J., Mucke, L., 2016. Network abnormalities and interneuron dysfunction in Alzheimer disease. Nat. Rev. Neurosci. 17, 777–792. https://doi.org/10.1038/nrn.2016.141

Pena-Ortega, F., Solis-Cisneros, A., Ordaz, B., Balleza-Tapia, H., Javier Lopez-Guerrero, J., 2012. Amyloid beta 1-42 inhibits entorhinal cortex activity in the beta-gamma range: role of GSK-3. Curr Alzheimer Res 9, 857–863.

Perkel, D.H., Gerstein, G.L., Moore, G.P., 1967a. Neuronal spike trains and stochastic point processes. I. The single spike train. Biophys. J. 7, 391–418. https://doi.org/10.1016/S0006-3495(67)86596-2

Perkel, D.H., Gerstein, G.L., Moore, G.P., 1967b. Neuronal spike trains and stochastic point processes. II. Simultaneous spike trains. Biophys. J. 7, 419–440. https://doi.org/10.1016/S0006-3495(67)86597-4

Sanchez, P.E., Zhu, L., Verret, L., Vossel, K.A., Orr, A.G., Cirrito, J.R., Devidze, N., Ho, K., Yu, G.-Q., Palop, J.J., Mucke, L., 2012. Levetiracetam suppresses neuronal network dysfunction and reverses synaptic and cognitive deficits in an Alzheimer's disease model. Proc. Natl. Acad. Sci. U.S.A. 109, E2895-2903. https://doi.org/10.1073/pnas.1121081109

Schevon, C.A., Weiss, S.A., McKhann, G., Goodman, R.R., Yuste, R., Emerson, R.G., Trevelyan, A.J., 2012. Evidence of an inhibitory restraint of seizure activity in humans. Nat Commun 3, 1060. https://doi.org/10.1038/ncomms2056

Siegle, J.H., López, A.C., Patel, Y.A., Abramov, K., Ohayon, S., Voigts, J., 2017. Open Ephys: an open-source, plugin-based platform for multichannel electrophysiology. J Neural Eng 14, 045003. https://doi.org/10.1088/1741-2552/aa5eea

Stark, E., Eichler, R., Roux, L., Fujisawa, S., Rotstein, H.G., Buzsáki, G., 2013. Inhibition-induced theta resonance in cortical circuits. Neuron 80. https://doi.org/10.1016/j.neuron.2013.09.033

Surges, R., Volynski, K.E., Walker, M.C., 2008. Is levetiracetam different from other antiepileptic drugs? Levetiracetam and its cellular mechanism of action in epilepsy revisited. Ther Adv Neurol Disord 1, 13–24. https://doi.org/10.1177/1756285608094212

Truccolo, W., Donoghue, J.A., Hochberg, L.R., Eskandar, E.N., Madsen, J.R., Anderson, W.S., Brown, E.N., Halgren, E., Cash, S.S., 2011. Single-neuron dynamics in human focal epilepsy. Nat. Neurosci. 14, 635–641. https://doi.org/10.1038/nn.2782

Verret, L., Mann, E.O., Hang, G.B., Barth, A.M.I., Cobos, I., Ho, K., Devidze, N., Masliah, E., Kreitzer, A.C., Mody, I., Mucke, L., Palop, J.J., 2012. Inhibitory interneuron deficit links altered network activity and cognitive dysfunction in Alzheimer model. Cell 149, 708–721. https://doi.org/10.1016/j.cell.2012.02.046

Vogl, C., Mochida, S., Wolff, C., Whalley, B.J., Stephens, G.J., 2012. The synaptic vesicle glycoprotein 2A ligand levetiracetam inhibits presynaptic Ca2+ channels through an intracellular pathway. Mol. Pharmacol. 82, 199–208. https://doi.org/10.1124/mol.111.076687

Vossel, K.A., Beagle, A.J., Rabinovici, G.D., Shu, H., Lee, S.E., Naasan, G., Hegde, M., Cornes, S.B., Henry, M.L., Nelson, A.B., Seeley, W.W., Geschwind, M.D., Gorno-Tempini, M.L., Shih, T., Kirsch, H.E., Garcia, P.A., Miller, B.L., Mucke, L., 2013. Seizures and epileptiform activity in the early stages of Alzheimer disease. JAMA Neurol 70, 1158–1166. https://doi.org/10.1001/jamaneurol.2013.136

Wyler, A.R., Ojemann, G.A., Ward, A.A., 1982. Neurons in human epileptic cortex: correlation between unit and EEG activity. Ann. Neurol. 11, 301–308. https://doi.org/10.1002/ana.410110311

Yang, X.-F., Weisenfeld, A., Rothman, S.M., 2007. Prolonged exposure to levetiracetam reveals a presynaptic effect on neurotransmission. Epilepsia 48, 1861–1869. https://doi.org/10.1111/j.1528-1167.2006.01132.x

Yoshiike, Y., Kimura, T., Yamashita, S., Furudate, H., Mizoroki, T., Murayama, M., Takashima, A., 2008. GABA(A) receptor-mediated acceleration of aging-associated memory decline in APP/PS1 mice and its pharmacological treatment by picrotoxin. PLoS ONE 3, e3029. https://doi.org/10.1371/journal.pone.0003029

Ziyatdinova, S., Gurevicius, K., Kutchiashvili, N., Bolkvadze, T., Nissinen, J., Tanila, H., Pitkänen, A., 2011. Spontaneous epileptiform discharges in a mouse model of Alzheimer's disease are suppressed by antiepileptic drugs that block sodium channels. Epilepsy Res. 94, 75–85. https://doi.org/10.1016/j.eplepsyres.2011.01.003

Ziyatdinova, S., Viswanathan, J., Hiltunen, M., Tanila, H., Pitkänen, A., 2015. Reduction of epileptiform activity by valproic acid in a mouse model of Alzheimer's disease is not long-lasting after treatment discontinuation. Epilepsy Res. 112, 43–55. https://doi.org/10.1016/j.eplepsyres.2015.02.005

Zott, B., Simon, M.M., Hong, W., Unger, F., Chen-Engerer, H.-J., Frosch, M.P., Sakmann, B., Walsh, D.M., Konnerth, A., 2019. A vicious cycle of β amyloid-dependent neuronal hyperactivation. Science 365, 559–565. https://doi.org/10.1126/science.aay0198

Figure legends

Figure 1. Representative histological sections from a transgenic APP/PS1 mouse; W02 antibody staining for Aβ deposits revealed plaques in the frontal somatosensory cortex (left) and two reconstructed electrode positions from successive recordings (right) (scale bars: left=100 µm, right 200 µm).

Figure 2. Increased LFP Power in APP/PS1 mice; Population average power from APP/PS1 mice and wild type controls (APP/PS1 n=4 mice, 6 sessions; WT n=3 mice, 4 Sessions). Black bar indicates significant Power differences from 6-28 Hz (permutation test at each Frequency p<0.05). Shaded areas indicate SEM.

*Figure 3. Decreased pyramidal cell firing rates in APP/PS1 mice A) Average action potential waveforms of all recorded putative pyramidal cells (blue) and interneurons (red) B) Spike width vs. valley to peak ratio of all recorded single cells, color-coded according to Gaussian mixture model classification. C) Average firing rates of putative pyramidal cells and interneurons in saline treated wild-type controls and APP/PS1 mice (n=228 (WT/Pyr); 386 (APP/PS1/Pyr); 35 (WT/Int); 45 (APP/PS1/Int); ** indicates p<0.01). Error bars represent SEM. D) Comparison between pyramidal cell firing rates in individual wild-type vs individual APP/PS1 mice (** indicates p<0.01 between groups (same as in C); Error bars represent SEM).*

*Figure 4. Theta & beta phase - pyramidal cell spike coherence is increased in APP/PS1 mice. A) Example periods from APP/PS1 (top) and WT (bottom) recording sessions, showing LFP (red), theta (green) and pyramidal cell firing (blue). Note that overall sparser spikes are clusters around theta troughs in APP/PS1 mice. B) APP/PS1 pyramidal cells are significantly more locked to theta (MRL= mean resultant length, ***indicates p<.001, n=228 (WT/Pyr); 386 (APP/PS1/Pyr)). Error bars represent SEM (left)Distribution of average firing phase of all significantly modulated WT(blue) and APP/PS1 (red) pyramidal cells (Rayleigh test for circular uniformity) (right). Green line on top indicates Theta phase. C) APP/PS1 pyramidal cells are significantly more locked to the ongoing beta oscillations than pyramidal cells in wild-type controls (MRL= mean resultant length, ***indicates p<.001, n=228 (WT/Pyr); 386 (APP/PS1/Pyr)). D) APP/PS1 pyramidal cells are not significantly more locked to the ongoing gamma oscillations than pyramidal cells in wild-type controls (30-100 Hz) (p=.75).*

*Figure 5. Levetiracetam restores pyramidal cell firing rates in APP/PS1 mice. A) Average firing rates of putative pyramidal cells and interneurons in APP/PS1 mice treated either with saline or levetiracetam injections (n=386 (APP/PS1/Pyr/Sal); 326 (APP/PS1/Pyr/Lev); 45 (APP/PS1/Int/Sal); 39 (APP/PS1/Int/Lev ;*** indicates p<0.001;Error bars represent SEM). B) Average firing rates in individual APP/PS1 mice treated with saline or levetiracetam (*indicates p<0.05; *** indicates p<0.001; Error bars represent SEM). C) Example sessions of pairwise correlations of simultaneously recorded neurons from one animal with saline (top) and levetiracetam (bottom) injections. Red and blue bar indicates interneurons and pyramidal cells. D) Average pairwise correlations of all simultaneously recorded pyramidal cells (blue), interneurons (red) and pyramidal – interneuron cell pairs (green) (*** indicates p<0.001; Error bars represent SEM) (right).*

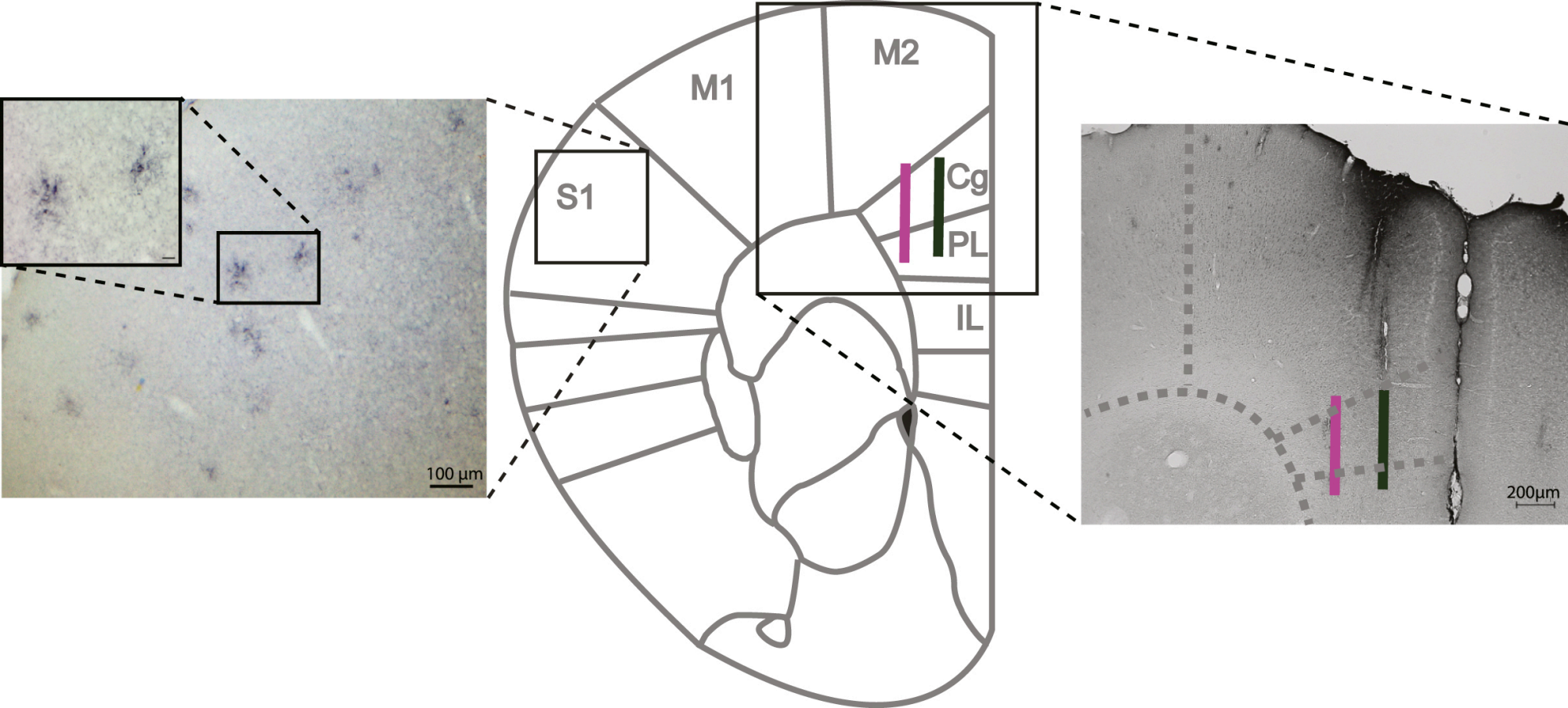
M1
M2
S1
Cg
PL
IL
100 µm
200µm

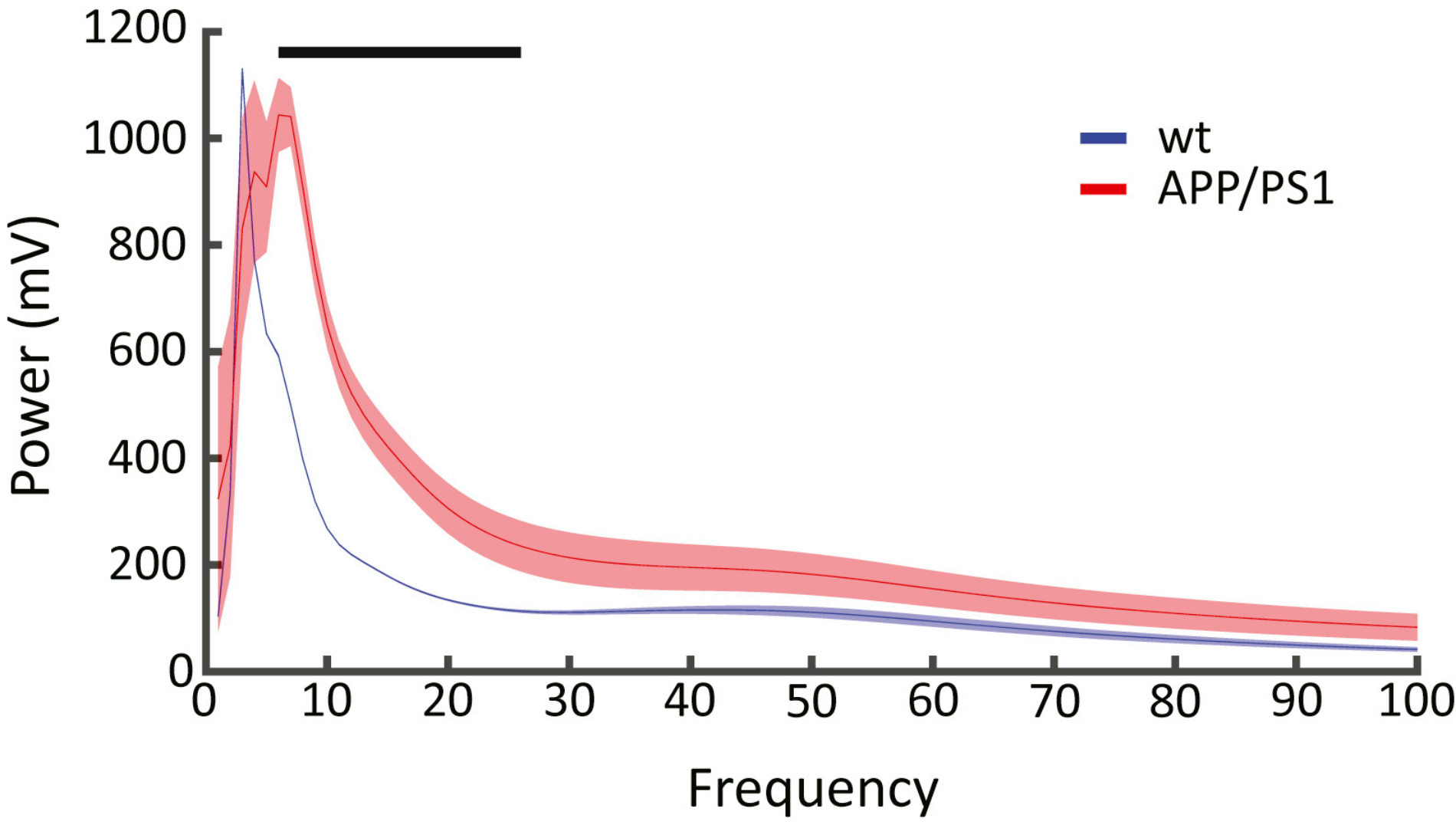
1200
1000
800
600
400
200
0
Power (mV)
0
10
20
30
40
50
60
70
80
90
100
Frequency
wt
APP/PS1

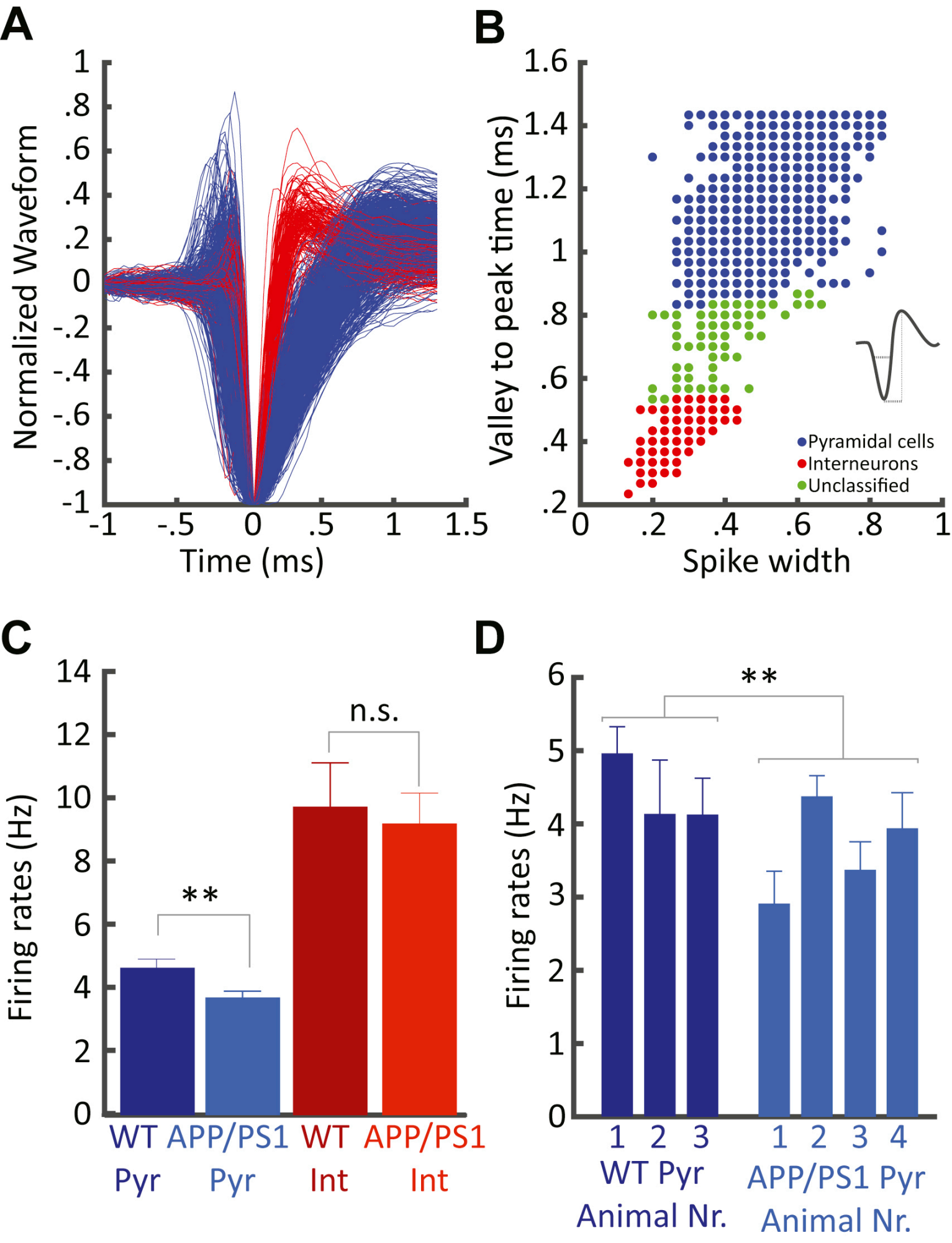
A
Normalized Waveform
Time (ms)
B
Valley to peak time (ms)
Spike width
Pyramidal cells
Interneurons
Unclassified
C
Firing rates (Hz)
**
n.s.
WT Pyr
APP/PS1 Pyr
WT Int
APP/PS1 Int
D
Firing rates (Hz)
**
1 2 3
WT Pyr
Animal Nr.
1 2 3 4
APP/PS1 Pyr
Animal Nr.

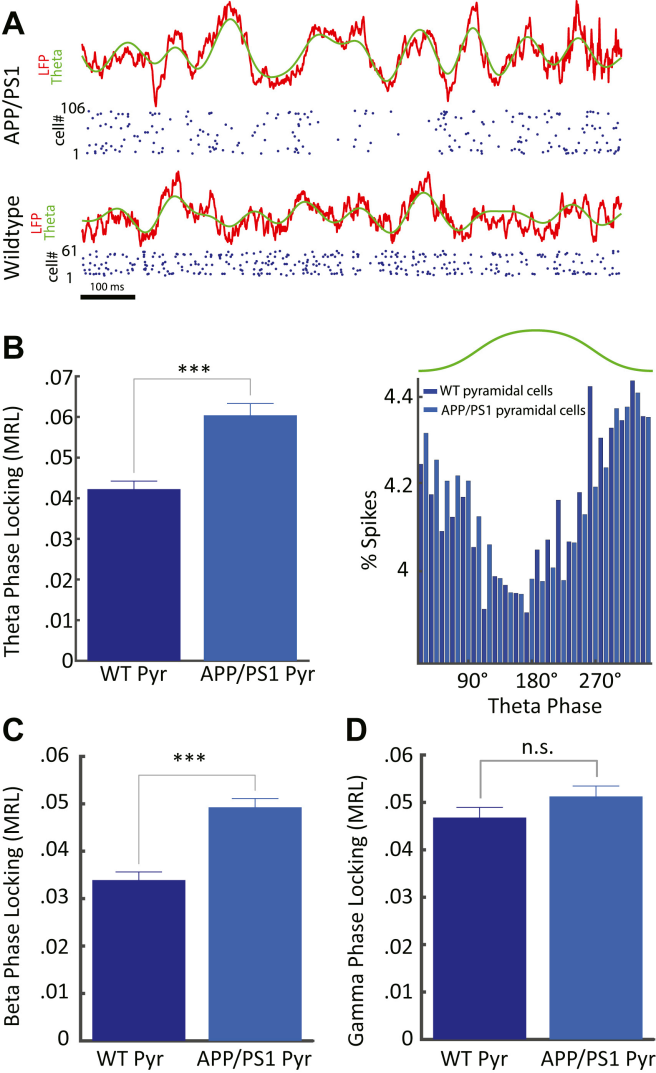
A
APP/PS1
LFP
Theta
106
cell#
1
Wildtype
LFP
Theta
61
cell#
1
100 ms
B
Theta Phase Locking (MRL)
.07
.06
.05
.04
.03
.02
.01
0
***
WT Pyr
APP/PS1 Pyr
WT pyramidal cells
APP/PS1 pyramidal cells
% Spikes
4.4
4.2
4
90°
180°
270°
Theta Phase
C
Beta Phase Locking (MRL)
.06
.05
.04
.03
.02
.01
0
***
WT Pyr
APP/PS1 Pyr
D
Gamma Phase Locking (MRL)
.06
.05
.04
.03
.02
.01
0
n.s.
WT Pyr
APP/PS1 Pyr

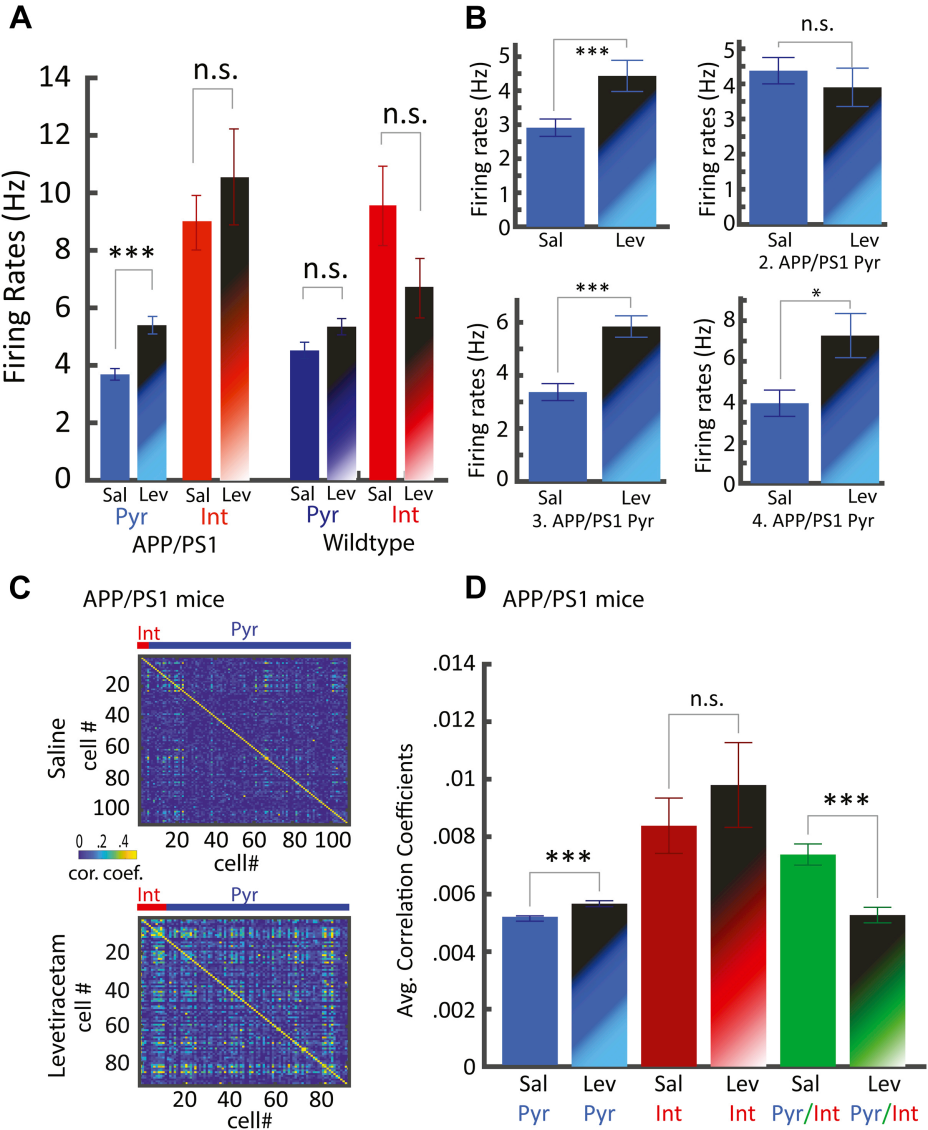
A
Firing Rates (Hz)
14
12
10
8
6
4
2
0
***
n.s.
n.s.
n.s.
Sal Lev Sal Lev Sal Lev Sal Lev
Pyr Int Pyr Int
APP/PS1
Wildtype
B
Firing rates (Hz)
***
Sal Lev
n.s.
Sal Lev
2. APP/PS1 Pyr
***
Sal Lev
3. APP/PS1 Pyr
*
Sal Lev
4. APP/PS1 Pyr
C
APP/PS1 mice
Int
Pyr
Saline
cell #
20
40
60
80
100
0 .2 .4
cor. coef.
20 40 60 80 100
cell#
Levetiracetam
20
40
60
80
20 40 60 80
cell#
D
APP/PS1 mice
Avg. Correlation Coefficients
.014
.012
.01
.008
.006
.004
.002
0
***
n.s.
***
Sal Lev Sal Lev Sal Lev
Pyr Pyr Int Int Pyr/Int Pyr/Int

Highlights

- 9 months old APP/PS1 mice exhibit increased theta and beta oscillations in the frontal cortex

- Pyramidal cell firing rates are significantly decreased but more phase-locked to ongoing LFP oscillations

- Levetiracetam treatment uncouples pyramidal cells and interneurons and elevates pyramidal cell firing rates

Jan L Klee: Conceptualization, Methodology, Formal analysis, Investigation, Writing – Original Draft, Writing – Review and Editing, Visualization, Project administration.

Amanda J. Kiliaan: Conceptualization, Resources, Writing – Original Draft, Writing – Review and Editing.

Arto Lipponen: Conceptualization, Methodology, Investigation, Writing – Original Draft, Writing – Review and Editing, Visualization, Supervision, Funding acquisition, Project administration.

Francesco P. Battaglia: Conceptualization, Methodology, Resources, Writing – Original Draft, Writing – Review and Editing, Supervision, Funding acquisition

1. The authors report no conflicts of interest. The manuscript is unpublished and not being offered for publication elsewhere.

2. The study was supported by the Säätiöiden post doc -pooli (The Finnish Cultural Foundation) to Dr. Arto Lipponen. Silicon probes were manufactured by IMEC (Leuven, Belgium) with funding from the European Union's Seventh Framework Programme (FP7/2007-2013) under grant agreement nr. 600925 (NeuroSeeker).

3. The manuscript is unpublished and not being offered for publication elsewhere.

4. The manuscript meets the guidelines for ethical conduct and report of research. All experiments were approved by the Dutch governmental Central Commissie Dierproeven (CCD) (10300) and conducted in accordance with the ARRIVE guidelines.

5. All authors have reviewed the contents of the manuscript being submitted, approve of its contents and validate the accuracy of the data.